Modern Chemistry
2014; 2(3): 19-28
Published online August 20, 2014 (http://www.sciencepublishinggroup.com/j/mc)
doi: 10.11648/j.mc.20140203.11
ISSN: 2329-1818 (Print); ISSN: 2329-180X (Online)

Synthesis and characterization of binary and ternary dioxouranium (VI) complexes with oxygen, Nitrogen and sulphur donor ligands

Abeer A. Faheim[1, 2]

[1]Chemistry Department, Faculty of Science (Girl's), Al-Azhar University, Nasr-City, Cairo, Egypt, P.O.Box 11754.
[2]Chemistry Department, College of Education and Science (Khurma), Taif University, Al-khurma, Taif, Sudia Arabia

Email address:
aafwafy@hotmail.com

To cite this article:
Abeer A. Faheim. Synthesis and Characterization of Binary and Ternary Dioxouranium (VI) Complexes with Oxygen, Nitrogen and Sulphur Donor Ligands. *Modern Chemistry.* Vol. 2, No. 3, 2014, pp. 19-28. doi: 10.11648/j.mc.20140203.11

Abstract: Mononuclear binary and ternary complexes of UO_2^{2+} ion with N-salicylidene-4-Aminotoluene-3-sulfonic acid as primary ligand and 8-hydroxyquinoline as coligand have been prepared. The elemental analysis, molar conductance, IR and solid reflectance spectra in addition to the magnetic moment measurements, thermal study, XRD and SEM analysis were utilized to investigate the coordination behavior of these complexes. From the investigation data, all complexes have metal to ligand ratio of 1:1 and 1:1:1 with octahedral and dodecahedral geometry for binary and ternary complexes, respectively and the force constant, F_{U-O} and bond length, R_{U-O} were calculated. The thermal behavior of these complexes was investigated and the thermal decomposition pathways have been postulated showing that the final product is metal or metal oxide. Antimicrobial properties of the complexes have also been examined against *Staphylococcus aureus* (ATCC 25923), *Streptococcus pyogenes* (ATCC 19615), *Pseudomonas fluorescens* (S 97), *Pseudomonas phaseolicola* (GSPB 2828), *Fusarium oxysporum* and *Aspergillus fumigatus*. The corrosion inhibition of aluminum specimens in acidic solution was studied by weight loss method. The ternary complex, $[UO_2(HL)(8\text{-Oqu})H_2O]$ was found to be exhibits excellent inhibitory activity against the different microorganisms in addition to its corrosion inhibition efficiency towards Al-specimens in acidic solution more than the binary complex, $[UO_2(HL)NO_3].2H_2O$.

Keywords: 8-Hydroxyquinoline, Mixed Ligand Complexes, Spectroscopic Characterization, Thermal Investigation, Acid Inhibition, Biological Study

1. Introduction

The actinides occupy the second row of the f-block on the periodic table, are strong electron acceptors and tend to interact with strong electron donors [1,2]. Of all the actinide ions, the uranyl ion $(UO_2)^{2+}$ has been the most thoroughly studied as it has the most stable oxidation state and can easily form complexes with various types of ligands [3,4]. The dioxouranium (VI) complexes with N and O donor Schiff bases have been the subject of many investigations, moreover, in the last few decades, mixed ligand complexes have been extensively studied in solution as well as in the solid state and the ternary complexes are found to be more stable than binary complexes [5,6]. These mixed ligand complexes are used in a number of fields like biological, analytical, agricultural industrial and therapeutic applications [7]. Accordingly we intend to report herein, the synthesis and characterization of ternary complexes using Schiff base ligand with nitrogen, oxygen and sulphur donor sites [8] as primary ligand and 8-hydroxyquinoline as coligand.

2. Experimental

2.1. Analysis and Physical Measurements

All chemicals used were of highest available purity, were BDH, Fluka, Sigma or Merck products. They are: 8-hydroxyquinoline, uranyl nitrate hexahydrates, lithium hydroxide monohydrate, absolute ethyl alcohol, acetone, diethylether, dimethylformamide. Concentrated hydrochloric acid was reagent grade and used as supplied. The Schiff base ligand, N-salicylidene-4-aminotoluene-3-

sulfonic acid (H_2L) has been described previously [8].

Microanalyses of carbon, hydrogen, nitrogen and sulfur contents were determined using a Perkin–Elmer 2408 CHN analyzer. Uranyl contents were determined gravimetric [9]. Melting or decomposition points were carried out on a melting point apparatus, Gallenkamp, England. Molar conductance measurements were measured in solutions of the metal complexes in DMF (10^{-3} M) using WTWD- 812 Weilheium-Conductivity meter model LBR, fitted with a cell model LTA100. IR spectra were recorded on a Perkin–Elmer FTIR type 1650 spectrophotometer using KBr discs. The solid reflectance spectra were recorded on a Jasco model V-550 UV–Vis spectrophotometer. TG–DSC measurements were carried out on a Shimadzu thermogravimetric analyzer using the TA-50 WSI program. X-ray powder diffraction analysis were carried out at ambient temperature with a Shimadzu 160D X-ray diffractometer using Cu-Kα radiation over the range ($4< 2\theta < 80$), with steps of 0.01^o and a step time of 2 s. Scanning electron microscopy (gold coating, Edwards Sputter Coater, UK) was performed using a Jeol 6310 (Jeol Instruments, Tokyo, Japan) system running at 5–10 keV. The agar-disk diffusion technique was followed to determine the activity of the synthesized compounds against some sensitive organisms [10]. Corrosion inhibition properties have been studied by weight loss measurements for aluminum specimens in 1.0 M HCl solution for different exposure periods (0.5–1.5h) at ambient temperature [11].

2.2. Preparation of the Binary Complex

(0.005 mol) of Uranyl nitrate hexahydrate dissolved in a least amount of distilled water was added to a mixture of (0.005 mol) $LiOH{\cdot}H_2O$ and (0.005 mol) H_2L in 40 ml ethanol. After complete addition, the reaction mixture was refluxed for 3 h with constant stirring to ensure the complete formation of metal complex. The precipitated solid complex was filtered, washed several times with 50% (v/v) ethanol–water followed by ethyl alcohol then diethyl ether and dried in vacuum desiccators over anhydrous $CaCl_2$.

2.3. Preparation of Ternary Complex

(0.005 mol) of Uranyl nitrate hexahydrate dissolved in a least amount of distilled water was added to a mixture of (0.005 mol) $LiOH{\cdot}H_2O$, (0.005 mol) H_2L and (0.005 mol) of 8-hydroxyquinoline as a coligand in 60 ml ethanol. After complete addition, the reaction mixture was refluxed for 4 h with constant stirring to ensure the complete formation of metal complex. The precipitated solid complex was filtered, washed several times with 50% (v/v) ethanol–water followed by ethyl alcohol then diethyl ether and dried in vacuum desiccators over anhydrous $CaCl_2$.

2.4. Weight Loss Measurements

Weight loss measurements were carried out using aluminum specimens from Aluminum Company of Egypt has a composition (wt %): Ti (0.006), Zn (0.002), Sb (0.010), Mg (0.002), V (0.005), Mn (0.001), Sn (0.002), Cu (0.003), Pb (0.001), Fe (0.159), Ni (0.002), Si (0.065), Cr (0.004) and balance Al with an regular shapes of 4 cm^2 cross-sectional area. Prior to experiment, the surface of aluminum specimens was abraded with the finest grade emery papers to mirror finish, washed thoroughly with acetone and distilled water and finally dried at room temperature. After weighing accurately, Al-specimens were immersed in 50 mL solution of 1.0 M HCl without and with the compounds under study (Schiff base ligand / metal complexes) acting as inhibitors at concentration 0.004 M for different exposure periods (0.5–1.5h) at room temperature. At the end of a run, the specimens were taken out, washed, dried and weighed accurately. Duplicate experiments were performed in each and the mean value of the weight loss has been reported [11].

2.5. Antimicrobial Screening

Eight pathogenic microbes were used to test the biological potentials of the newly synthesized binary and ternary complexes. They were *Staphylococcus aureus* (ATCC 25923) and *Bacillus subtilis* (ATCC 6635) as Gram-positive bacteria; *Escherichia coli* (ATCC 25922) and *Salmonella typhimurium* (ATCC 14028) as Gram-negative bacteria in addition to Yeast; *Candida albicans* (ATCC 10231) and Fungus; *Aspergillus fumigatus*. The antibiotics; *Cephalothin* and *Chloramphencol,* were used as standard references for Gram-positive bacteria and Gram-negative bacteria, respectively, while *Cycloheximide* was used as standard reference in the case of yeasts and fungi. Antimicrobial activity was determined using the standardized disk–agar diffusion method [10] described below:

The tested compounds were dissolved in DMF, which has no inhibition activity to get concentrations of 0.5 and 1 mg/mL in DMF. The test was performed on medium potato dextrose agar (PDA), which contains an infusion of 200 g potatoes, 6 g dextrose, and 15 g agar. Uniform size filter paper disks (3 disks per compound) were impregnated by an equal volume (10 µL) from the specific concentration of dissolved tested compounds and carefully placed on inoculated agar surface. After incubation for 36 h at 27^oC in the case of bacteria and for 48 h at 24^oC in the case of fungi, the inhibition zone diameter produced by these compounds against the particular test organism determined the antimicrobial activity of the compound. The mean value obtained for three individual replicates was used to calculate the zone of growth inhibition of each sample. The activity of tested compounds was categorized as (a) low activity = mean of zone diameter is ≤ 1/3 of mean zone diameter of control, (b) intermediate activity = mean of zone diameter ≤ 2/3 of mean zone diameter of control and (c) high activity = mean of zone diameter >2/3 of mean zone diameter of control. Additionally, the % Activity Index for the tested compounds was calculated [12].

3. Results and Discussion

3.1. Elemental Analysis

The elemental analysis results for the metal complexes are in good agreement with the calculated values (Table 1) showing that the complexes have metal to ligand stoichiometry of 1:1 and 1:1:1 for binary and ternary complexes, respectively with suggested formula as : $[UO_2(HL)NO_3].2H_2O$ (1) and $[UO_2(HL)$ (8-Oqu)$H_2O].2H_2O$ (2) that represented in Fig.1.

Table 1. *Analytical data and some physical properties of the binary and ternary complexes*

Compd. No[(a)] Emperical formula	Color	M.P (°C)	Conductance value ($\Omega^{-1}mol^{-1}cm^2$)	μ_{eff} (B.M)	Elemental analysis, found (calcd. %)				
					C	H	N	S	M
(1) $[UO_2(HL)NO_3].2H_2O$ $UO_2C_{14}H_{12}N_2O_7S.2H_2O$; 658.42	Pale orange	> 300	22	Dia.	25.33 (25.54)	1.91 (1.84)	4.48 (4.25)	4.61 (4.87)	36.42 (36.15)
(2) $[UO_2(HL)($ 8-Oqu) $H_2O].2H_2O$ $UO_2C_{23}H_{18}N_2O_5S.3H_2O$; 758.59	Darck orange	> 300	48	Dia.	36.88 (36.41)	2.76 (2.40)	3.21 (3.69)	4.50 (4.23)	31.09 (31.38)

[(a)]HL Represent the deprotonated form of Schiff base ligand 8-Oqu Represent the deprotonated form of 8-hydroxyquinoline.
[(b)]Conductance value measured in DMF.

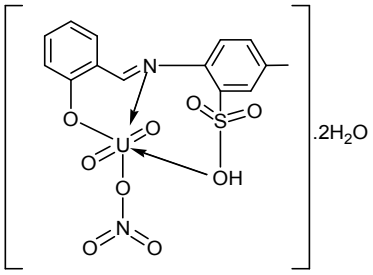

$[UO_2(HL)NO_3].2H_2O$ (1)

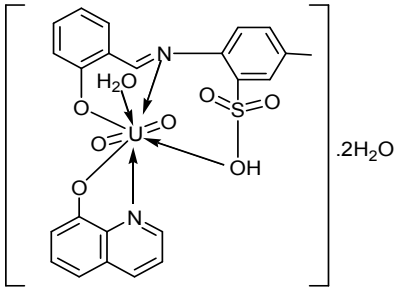

$[UO_2(HL)($ 8-Oqu) $H_2O].2H_2$ (2)

Figure. 1. *Suggested structure of binary and ternary complexes (1,2), respectively*

3.2. Conductivity Measurements

The molar conductance values of the metal complexes in DMF (10^{-3} M solution) were measured at room temperature and the results are listed in Table 1. It is concluded from the results that the metal complexes (1,2) were found to have molar conductance values 22 and 48 $\Omega^{-1}cm^2mol^{-1}$, respectively which indicates that they are non electrolytic in nature and there is no counter ion present outside their coordination sphere [13].

3.3. Infrared Spectroscopy

The main IR characteristic stretching frequencies of the binary complex, ternary complex and free ligand (H_2L), along with their proposed assignments are given in Table 2. The IR spectra of metal complexes show a shift of the ν(C=N) to lower frequency by 23–21 cm^{-1} compared with the free ligand band at 1651cm^{-1}. This shift indicates coordination of the azomethine group to the metal ions, moreover the coordination of nitrogen to the metal ions would be expected to reduce the electron density of the azomethine link and thus cause a shift in the ν(C=N) group [14]. In the far IR spectra of all complexes, the non-ligand bands observed at 455–410 cm^{-1} region assigned to ν(M–N) stretch [15]. The disappearance of the free ligand ν(OH) band around 3425 cm^{-1} in the spectra of all complexes indicating deprotonation of Schiff base prior to coordination, on the other hand, the ν(C–O), which occur at 1304 cm^{-1} for the ligand, was moved to higher frequencies, (1396 –1312 cm^{-1}) by 92–8 cm^{-1} after complexation, this shift confirms the participation of phenolic oxygen of the ligand in C–O–M bond formation [16,17]. Conclusive evidence regarding the bonding of oxygen to the metal ions is provided by the occurrence of bands at 525–502 cm^{-1} region due to ν (M–O) [18]. Moreover, the characteristic vibrations of ν(SO_3 asym), ν(SO_3 sym) and ν(SO_2–OH) at 1204, 1018 and 2530 cm^{-1} in the free ligand are located around 1157-1155, 1072-995 and 2631-2523 cm^{-1}, respectively in the metal complexes confirming the involvement of sulphonato group in coordination [8]. IR spectra also display two strong bands at 926 and 903 cm^{-1} for the complexes (1,2), respectively assigned to ν_3(O=U=O) vibration. The force constant ($F_{U=O}$) and the bond length (R_{U-O}) were calculated. The calculated bond length values are 7.0632 and 6.7516 mdyn / ˚A, while the calculated force constant values are 1.7329 and 1.7414 ˚A for the UO_2(II) complexes, (1,2), respectively [19,20]. These values agree well with previously reported values for various uranyl complexes. In the mixed 8-hydroxyquinoline complexes (2), the broad stretching vibration at 3242 cm−1 due to O–H of the free 8-HQ was absent, suggesting formation of the M–O bond with 8-hydroxyquinolate, whereas the strong band at 1586 cm−1 due to stretching of the (C=N) group shifted to 1535 cm−1 on coordination suggesting that the lone pair on nitrogen is

involved in formation of a bond with metal [21]. Thus 8-hydroxyquinolate in this complex is monobasic bidentate chelating. Additionally, IR spectrum of complex (1) shows three bands at 1443, 1281 and 1072 cm−1 attributed to unidentate coordination of nitrate [22]. Finally, the assignment of the nature of water molecules associated with the complex formation under study was much more complicated as ligand vibrations interfere in this region. The thermal data confirms the nature of water molecule to be lattice/coordinated. The thermal study will be discussed in detailed manner later.

Table 2. *Infrared wave numbers (cm^{-1}) and tentative band assignments for the binary and ternary complexse*

Compd. No[(a)]	ν(C=N)	ν(C–O) Phenolic	V(SO_3)	V(SO_2-OH)	V(M-O)	V(M-N)	Other bands[(b)]
H_2L	1651	1304	1204, 1018	2530	-	-	3425 ν(OH) phenolic
(1)	1628	1312	1157, 995	2523	502	410	926 ν_3(O=U=O) and 1443; 1281; 1072 ν(NO_3 coordinate).
(2)	1630	1396	1155, 1072	2631	525	455	903 ν_3(O=U=O) and 1535(Qu.moiety)

[a]represent the complex number as in table 1.
[b]Qu represent quinoline moiety

3.4. Electronic Spectra

The electronic reflectance spectra of the metal complexes (1,2) have been recorded in the 800–200 nm range. The spectra showed new absorption band at 490 and 485 nm for complexes (1,2), respectively attributed to a charge transfer transition from the ligand to uranium ion indicating the formation of uranyl complexes. Additionally, the magnetic moment measurement suggested that the complexes are diamagnetic as expected with coordination number 6 and 8 and exists in octahedral and dodecahedral geometry, respectively [23-25].

3.5. Thermal Analyses (TG-DSC) of the Complexes

The results of TG-DSC analyses of the metal complexes, (1,2), Figs.2,3 as the decomposition stages, temperature ranges, decomposition products, the found and calculated weight loss as well as the probable residue and heat of reaction are given in Table 3. The results show good agreement with the previous suggested formulae of the complexes and revealed the following:

Table 3. *Thermal analyses data (TG-DSC) for binary and ternary complexes*

Compd. No Emperical formula	Temp. Range (°C)	% Weight loss Found (Calcd.)	Lost fragment	Probable residue Found/(Calcd.)	DSC peak (°C)		
					Endo	Exo	*ΔH* (J/g)
	47-362	5.67(5.47)	$2H_2O$ (hyd.)	$UO_2C_{14}H_{12}N_2O_7S$	86		-60.82
(1) $[UO_2(HL)NO_3].2H_2O$	363-412	7.33(6.99)	NO_2	$UO_2C_{14}H_{12}NO_5S$	104		-53.61
$UO_2C_{14}H_{12}N_2O_7S.2H_2O$	414-498	19.74(19.15)	NO_2 and SO_3	$UO_2C_{14}H_{12}$	360		-32.44
	499-719	31.88(32.24)	O_2, HC≡CH and C_6H_5-C_6H_5	U; 35.38(36.15)	459		-6.49
	44-324	11.92(11.34)	$2H_2O$ (hyd.), H_2O (coord.) and O_2	$UO_2C_{23}H_{18}N_2O_3S$	104		-66.12
(2) $[UO_2(HL)(8\text{-}Oqu)$	324-389	4.73(4.22)	O_2	$UO_2C_{23}H_{18}N_2OS$	399		33.71
$H_2O].2H_2O$	389-545	31.48(31.42)	C_6H_5SH and $C_{10}H_8$	$UO_2C_7H_4N_2O$	453	279	-20.44
$UO_2C_{23}H_{18}N_2O_5S.3H_2O$	545-686	13.50(13.85)	CO, HCN and HC≡C-C≡CH	UO_2CHN	523		-20.49
	687-776	2.62(3.56)	HCN	UO_2; 35.75(35.60)			-14.44

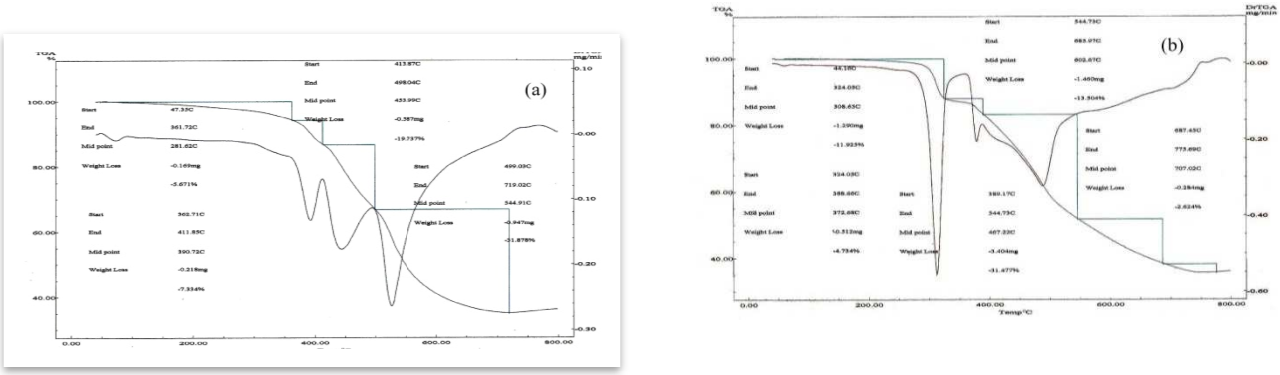

Figure 2. *TG- thermograme of (a) binary and (b) ternary complexes (1,2), respectively*

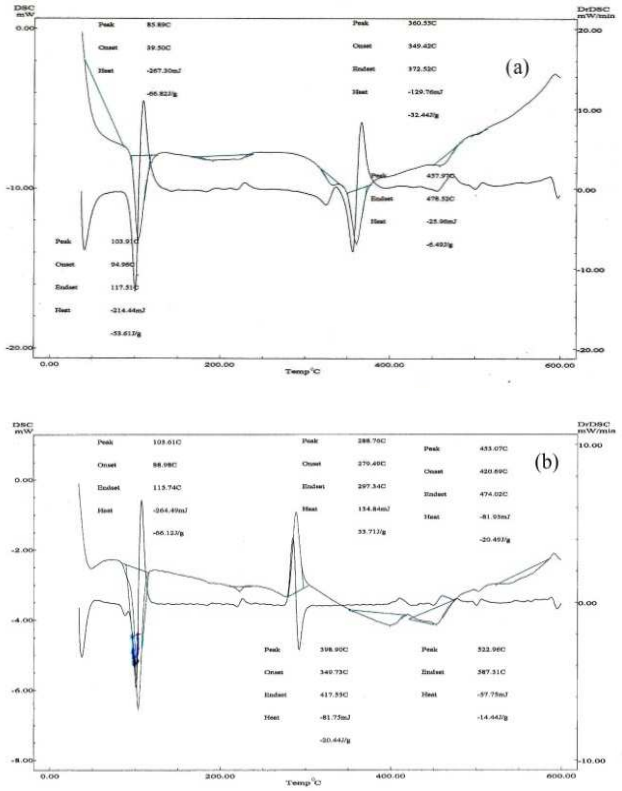

Figure 3. *DSC- thermograme of (a) binary and (b) ternary complexes (1,2), respectively*

$[UO_2(HL)NO_3].2H_2O$ (1) exhibits four steps of decomposition process from 47-719 ^{0}C. The initial weight loss of 5.67% (calcd. 5.47%) in the temperature range 47-362 ^{0}C is due to the loss of two hydrated water molecules. The loss of crystal water molecules in this complex was accompanied by an endothermic peak at 86 ^{o}C with ΔH -60.82 J/g. The next weight loss of 7.33% (calcd. 6.99%) in the range 363-412 ^{0}C attributed to a loss of NO_2 and accompanied by an endothermic peak at 104 ^{o}C with ΔH -53.61 J/g. The third stage within the temperature range 414-498 ^{o}C is related to the evolution of NO, O_2 and SO_2 with a found mass loss of 19.74% (calcd. 19.15%) and accompanied by an endothermic peak at 360 ^{o}C with ΔH -32.44 J/g. The final stage between 499-719 ^{o}C, represents the loss of O_2, HC≡CH and C_6H_5-C_6H_5 with a found mass loss of 31.88% (calcd. 32.24%) and accompanied by an endothermic peak at 459 ^{o}C with ΔH -6.49 J/g. The remaining residue is 35.38%, corresponding to formation of U- metal (calcd. 36.15%).

$[UO_2(HL)($ 8-Oqu) $H_2O].2H_2O$ (**2**) exhibits five steps of decomposition process from 44-776 ^{0}C. The initial weight loss of 11.92% (calcd. 11.34%) in the temperature range 44-324 ^{0}C is due to the loss of two hydrated water molecules, one molecule of coordinated water and O_2. This step was accompanied by an endothermic peak at 104 ^{o}C with ΔH -66.00 J/g. The next weight loss of 4.73% (calcd. 4.22%) in the range 324-389 ^{0}C attributed to a loss of O_2 and accompanied by an exothermic peak at 279 ^{o}C with ΔH 33.71 J/g. The third stage within the temperature range 389-545 ^{o}C is related to the evolution of C_6H_5SH and $C_{10}H_8$ with a found mass loss of 31.48% (calcd. 31.42%) and accompanied by an endothermic peak at 399 ^{o}C with ΔH -20.44 J/g. The fourth stage between 545-686 ^{o}C, represents the loss of CO, HCN and HC≡C-C≡CH with a found mass loss of 13.50% (calcd. 13.85%) and accompanied by an endothermic peak at 453^{o}C with ΔH -20.49 J/g. The final step is due to loss of HCN with a found mass loss of 2.62% (calcd. 3.56%) at temperature range 687-776 ^{o}C and accompanied by an endothermic peak at 523 ^{o}C with ΔH -14.44 J/g. The remaining residue is 35.75%, corresponding to the formation of UO_2 (calcd. 35.60%).

The sequence of the thermal decomposition process for the for binary and ternary complexes (1,2), respectively is summarized in Scheme 1 and the results obtained are in good agreement with the theoretical formula suggested from the elemental analysis.

3.6. Powder X-Ray Diffraction Characterization

The powder X-ray diffraction patterns of the metal complexes have been recorded in a scanning range of 5–80◦ (2θ) and depicted in Fig.4. Table 4 shows the observed diffraction data, i.e., inter planar spacing d (Å), relative intensities (I/I_0) and (2θ). From the patterns plotted in Fig. 2, we can observe that the diffraction peaks of all metal complexes, in terms of location, numbers or intensity are different from the ligand [8] indicating that the reaction produced a new crystalline phase, that is, the complex has been formed [26].

3.7. Scanning Electron Microscopy Analysis

Scanning electron microscope technique (SEM) gives a general perception about the microstructure, surface morphology and particle size of the compounds [27]. The scanning electron micrograph of Schiff base ligand and its uranyl complexes, (1,2) at room temperature depicted in Fig.5(a- c). and indicate that Schiff base ligand differ significantly from that of its complexes due to the metal ion, moreover, the surface morphology of metal complexes changes as a result of quinoline moiety [28].

3.8. Corrosion inhibition study

The weight loss method of monitoring corrosion rate is useful because of its simple application and reliability [29]. Therefore, a series of weight loss measurements were carried out after exposure period of 0.5, 1.0 and 1.5 h immersion in 1.0 M HCl at ambient temperature in the absence and presence of 0.004 M of the Schiff base ligand and its metal complexes (1,2) acting as inhibitors.

Table 4. *X-ray diffraction data of for binary and ternary complexes*

Peak no.	(1) $[UO_2(HL)NO_3].2H_2O$			(2) $[UO_2(HL)(8\text{-Oqu})\ H_2O].2H_2O$		
	d(A°)	Intensity (%)	2θ	d(A°)	Intensity (%)	2θ
1	11.91	100.00	7.42	12.73	49.38	6.94
2	6.53	19.84	13.56	11.96	77.05	7.39
3	5.94	13.84	14.91	7.38	66.04	11.99
4	5.55	5.98	15.96	6.50	28.81	13.61
5	4.88	14.68	18.16	6.06	20.83	14.62
6	4.74	10.15	18.71	3.58	100.00	24.85
7	3.95	11.11	22.47	3.50	41.53	25.44
8	3.65	12.90	24.34	3.22	75.62	27.66
9	3.58	22.94	24.85	3.16	43.18	28.22
10				2.57	14.80	34.85
11				2.04	17.49	44.45
12				1.96	15.93	46.25

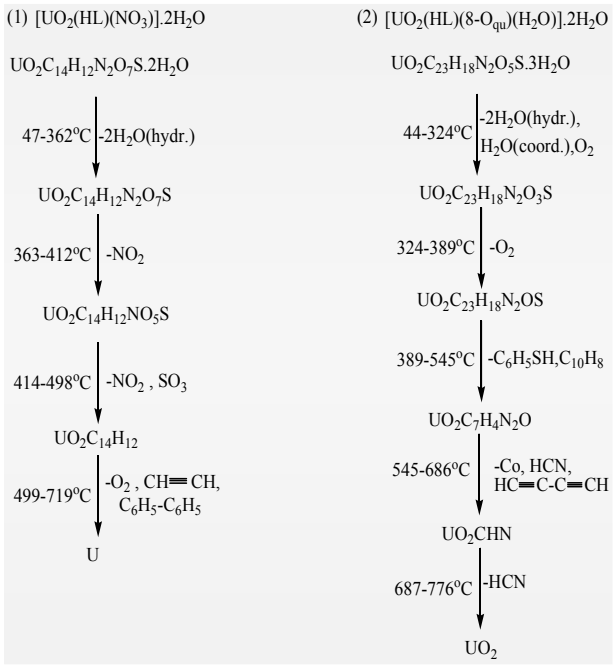

Scheme 1. *The thermal decomposition sequence for binary and ternary complexes (1,2), respectively*

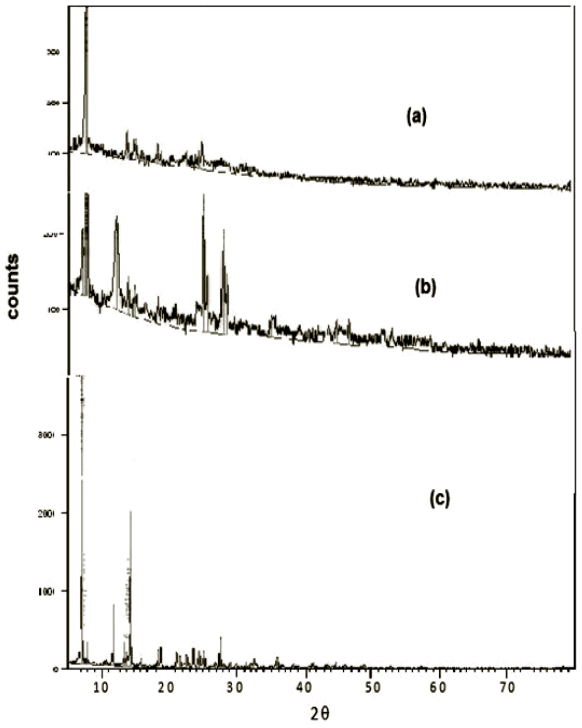

Figure 4. *XRD diagram of (a) binary complex, (b) ternarycomplex and (c)) H_2L ligand respective*

Table 5. *Corrosion parameters data for Al-specimens in absence and existence of corrosion inhibitors at ambient temperature after 0.5, 1.0 and 1.5h*

Inhibitor name	Weight loss, inhibition efficiency (%) and degree of surface coverage (θ)					
	after 0.5h		after 1.0h		after 1.5h	
	W(mg/cm^2)	IE (%)	W(mg/cm^2)	IE (%)	W(mg/cm^2)	IE (%)
Blank[(a)] *	1.65	-	3.48	-	5.78	-
H_2L	1.54	6.67 (0.07)*	2.89	16.95(0.17)	3.50	39.45(0.39)
(1)	1.31	20.61(0.21)	2.48	28.73(0.29)	2.81	51.38(0.51)
(2)	1.00	39.39(0.39)	1.79	48.56(0.48)	2.03	64.88(0.65)

[(a)]1M HCl

*The values in parentheses are that of degree of surface coverage.

When Al-specimens were immersed in 1.0 M HCl after exposure period of 0.5, 1.0 and 1.5 h, it suffered a weight loss of 1.65, 3.48 and 5.78mg cm^{-2}, respectively. A reduction in weight loss of the metal coupons in the presence of the inhibitors was observed compared to the blank, this indicates that the additives inhibit the corrosion of Al-specimens in the aggressive solution; (1.0 M HCl) [30]. Table 5 represents the corrosion inhibition efficiencies (% *IE*) of the synthesized inhibitors on the Al-specimens corrosion in 1.0 M HCl solution at ambient temperature. The extent of covering the metal surface by inhibitor molecules can be expressed in term of the surface coverage (θ) which represents the degree of arrangement of inhibitor molecules on the metal surface [31,32]. The relation between the different parameters was given in Figs.6,7 and revealed that the presence of the Schiff base ligand or its metal complexes in the aggressive solution inhibited the corrosion of Al-specimens and such inhibition may be attributed to larger coverage of metal surface with inhibitor molecules as a result to the accumulation of the inhibitor molecules onto the metal surface and protective film formation on the metal surface which decreases the interaction between the acidic medium and the metal surface [33]. Moreover, the ternary complex (2), showed comparatively enhanced inhibition efficiency than binary complex (1) or the Schiff base ligand may be due to presence of more functional groups as a result of the quinoline moiety [34].

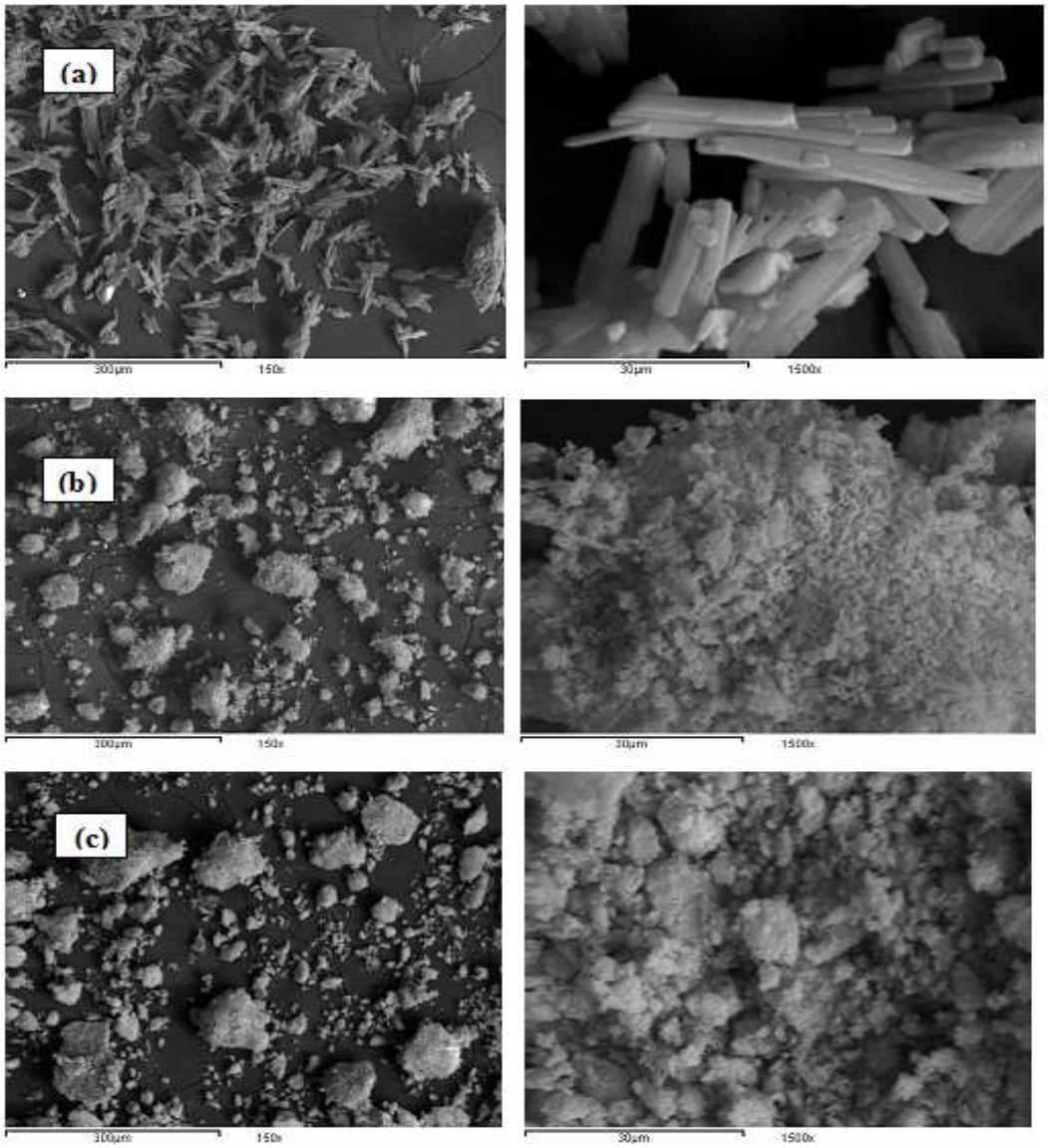

Figure. 5. *SEM photographs at 150 and 1500 magnifications of: (a) Schiff base ligand,(b) binary complex and (c) ternary complex,respectively*

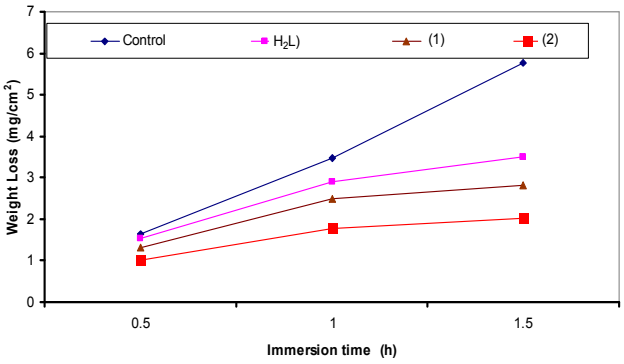

Figure. 6. *Weight loss against time for Al-specimens corrosion in 1.0M HCl in absence and presence of 0.004M of corrosion inhibitors*

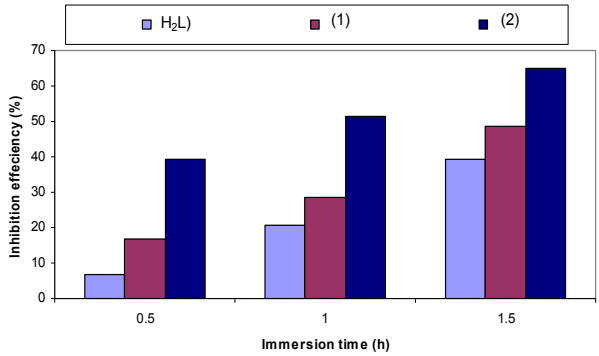

Figure 7. *Variation of inhibition efficiency (%) with immersion time in 1.0 M HCl in absence and presence of 0.004M of corrosion inhibitors*

3.9. Antimicrobial Assay

The antimicrobial activities of the newly synthesized complexes were tested in vitro against series of organisms to increase the chance of detecting antibiotic principles in tested materials. The activity was determined by measuring the inhibition zone diameter values (mm) of the complexes against the organisms. The screening data in addition to the calculated percent activity index are given in Table 6 and are graphically presented in Fig. 8(a,b). Analyzing the tabulated results show the following:

a) The complexes show a significant degree of antimicrobial activity against the tested organisms and the activity increases as the concentration of the complexes increases [35]. Both the uranyl complexes (1,2) have remarkable activity against all types of bacteria, yeasts and fungi. They display high activity (mean of zone diameter is >2/3 of mean zone diameter of reference standard) against *Salmonella typhimurium*, intermediate activity (mean of zone diameter is ≤ 2/3 of mean zone diameter of reference standard) against *Staphylococcus aureus* and *Bacillus subtilis* and display low activity (mean of zone diameter is ≤ 1/3 of mean zone diameter of reference standard) against *Escherichia Coli, Candida albicans* and *Aspergillus fumigates*.

b) The ternary complex (2) has a higher degree of activity than the binary complex (1) against all strains of organisms may be due to the increase in the functional group as a result to quinoline moiety [21].

c) The ternary complex (2) showed excellent inhibitory activity against the growth of the *Salmonella typhimurium*, it displays a comparable value to the standard.

These studies reveal that the ternary uranyl complex (2) can be used as potential chemotherapeutic agent and hold much promise in the field of drug discovery.

4. Conclusions

Binary and ternary complexes of UO_2(II) ion have been synthesized and their structural situation elucidated by various instrumental techniques. An octahedral and dodecahedral geometries were achieved around UO_2(II) in binary and ternary complexes, respectively. The bioactivity of these complexes in addition to their corrosion inhibition properties was studied. $[UO_2(HL)(8\text{-Oqu})H_2O].2H_2O$ (**2**) exhibits biological effect and corrosion inhibition properties higher than $[UO_2(HL)NO_3].2H_2O$ (**1**) may be due to quinoline moiety.

Table 6. *Antimicrobial screening results of the binary and ternary uranyl complexes*

Organism	Gram - positive bacteria				Gram - negative bacteria				Yeasts		Fungi	
	Staphylococcus aureus **(ATCC 25923)**		***Bacillus subtilis*** **(ATCC 6635)**		***Salmonella typhimurium*** **(ATCC 14028)**		***Escherichia coli*** **(ATCC 25922)**		***Candida albicans*** **(ATCC 10231)**		***Aspergillus fumigatus***	
Conc. Sample	**1 mg/mL**	**0.5 mg/mL**	**1 mg/mL**	**0.5 mg/mL**	**1 mg/mL**	**0.5 mg/mL**	**1 mg/mL**	**0.5 mg/mL**	**1 mg/mL**	**0.5 mg/mL**	**1 mg/mL**	**0.5 mg/mL**
(1)	20(57)	15(58)	19(54)	13(52)	25(69)	21(75)	10(26)	8(30)	9(26)	7(25)	11(30)	7(27)
(2)	23(66)	17(65)	22(63)	14(56)	30(83)	26(93)	13(34)	9(33)	11(31)	9(32)	12(32)	9(35)
DMF	0	0	0	0	0	0	0	0	0	0	0	0
R.S	35	26	35	25	36	28	38	27	35	28	37	26

- The test was done using the agar–disc diffusion method and % Activity indices are in parentheses.
- R.S; Reference standard : *Chloramphencol* and *Cephalothin* were used as standard references for Gram positive bacteria and Gram negative bacteria, respectively and *Cycloheximide* was used as standard reference in case of yeasts and fungi.
- Inhibition values: (a) low activity = diameter zone is ≤ 1/3 of mean zone diameter of control, (b) intermediate activity = diameter zone is ≤ 2/3 of mean zone diameter of control, (c) high activity = diameter zone is >2/3 of mean zone diameter of control and (e) -No effect.

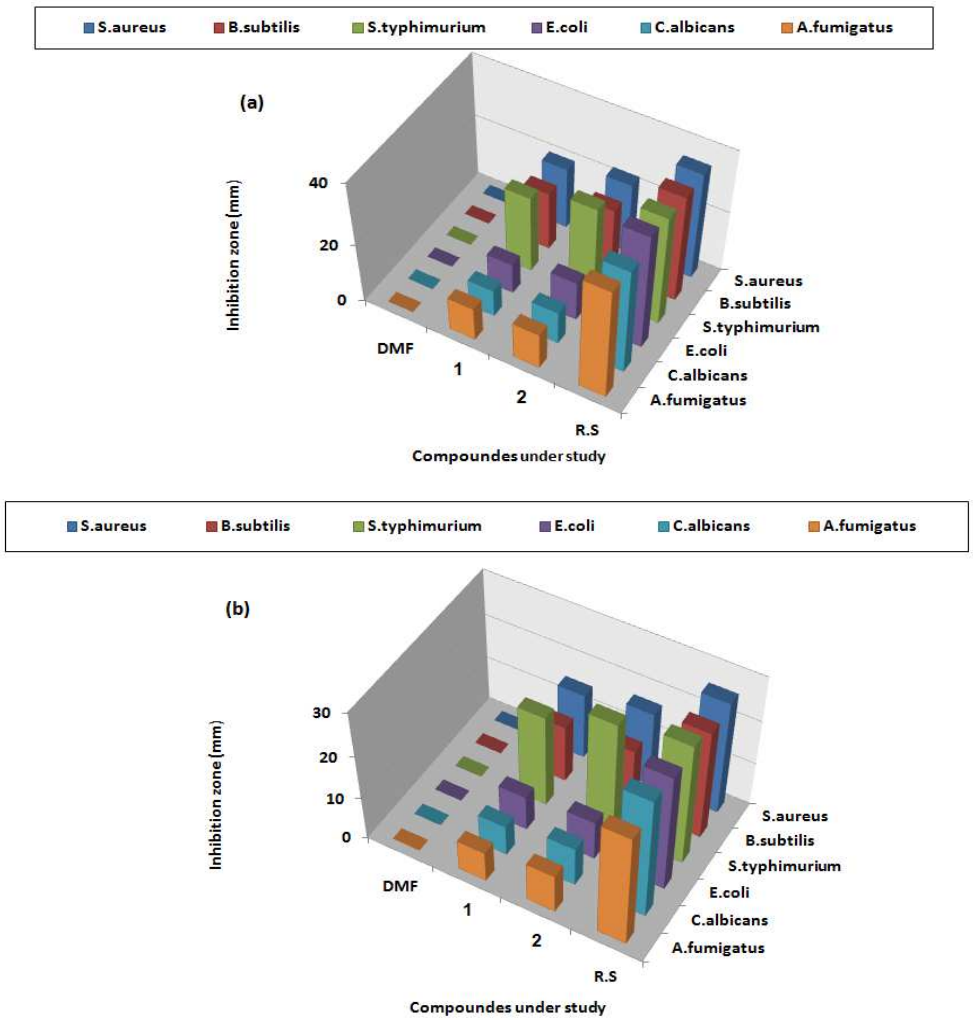

Figure. 8. *Antimicrobial activity of metal complexes towards different organisms at (a) higher concentration and (b) lower concentration, respectively*

References

[1] L.S. Natrajana, A.N. Swinburnea, M.B. Andrewsa, S. Randalla and S. L. Heatha, Coord. Chem. Rev., 2014, 267, 171–193.

[2] J.P. Dognon, Coord. Chem. Rev., 2014, 266, 110–122.

[3] R.J. Baker, Chem. Eur. J., 2012, 18, 16258 – 16271.

[4] S. D. Houwer and C. G. Walrand, J. Alloys Compd., 2001, 323–324, 683–687.

[5] S.K. Gupta, N. Sen and R. J. Butcher, Polyhedron, 2014, 71, 34–41.

[6] A.Z. El-Sonbati, M. A. Diab, A. A. El-Bindary, M. I. Abou-Dobara and H. A. Seyam, Spectrochim. Acta Part A, 2013, 104, 213–221.

[7] J. Dharmaraja, T. Esakkidurai, P. Subbaraj and S. Shobana, Spectrochim. Acta Part A, 2013, 114, 607-621.

[8] A.A. Faheim, S.N. Abdou and Z. H. Abd El-Wahab, Spectrochim. Acta Part A, 2013, 105, 109-124.

[9] M. Shebl, Spectrochim. Acta Part A, 2014, 117, 127-137.

[10] M. Shebl, S. M. E. Khalil and F. S. Al-Gohani, J. Mol. Struct., 2010, 980, 78-83.

[11] X. Li, S. Deng and H. Fu, Corros. Sci., 2012, 62, 163–175.

[12] M. Aljahdali, Spectrochim. Acta Part A, 2013, 112, 364-376.

[13] J. F. Wang, N. Ren, F. T. Meng, J. J. Zhang, Thermochim. Acta., 2011, 512, 118-123.

[14] Z. H. Abd El-Wahab, Spectrochim. Acta Part A, 2007, 67, 25-38.

[15] H. A. El-Boraey, F. A. El-Saied and S. A. Aly, J. Therm. Anal. Calorim. 2009, 96, 599–606.

[16] A. A. Nejo, G. A. Kolawole and A. O. Nejo, J. Coord. Chem., 2010, 63, 4398-4410.

[17] A. Manimaran and C. Jayabalakrishnan, Synth. React. Inorg. Met-Org. Nano-Met. Chem., 2010, 40, 116-128.

[18] N. Raman and A. Selvan, J. Mol. Struct., 2011, 985, 173-183.

[19] M. N. Abd El-Hady, R. R. Zaky, K. M. Ibrahim and E. A. Gomaa, J. Mol. Struct., 2012, 1016, 169–180.

[20] A. A. Ibrahim, A. M. Adel, Z. H. Abd El–Wahab and M. T. Al–Shemy, Carbohydr. Polym., 2011, 83, 94–115.

[21] Z. H. Abd El-Wahab, J.Coord. Chem., 2008, 61, 3284–3296.

[22] Z. H. Abd El-Wahab, M. M. Mashaly and A. A. Faheim, Chem. Pap., 2005, 59, 25-36.

[23] S. A. Sadeek, M. S. El-Attar and S. M. Abd El-Hamid, J. Mol. Struct., 2013, 1051, 30–40.

[24] O. M. I. Adly, Spectrochim. Acta Part A., 2011, 79, 1295–1303.

[25] A. A. Faheim, Spectrochim. Acta Part A., 2012, 88, 10– 22

[26] J. Wanga, F. Mengc, S. Xud, X. Liua and J. Zhanga, Thermochim. Acta., 2011, 521, 2– 8

[27] F. A. Al-Saif and M. S. Refat, J. Therm. Anal. Calorim., 2013, 111, 2079–2096.

[28] E. H. El-Mossalamy, F. M. Al-Nowaiser, S. A. Al-Thabaiti, A. O. Al-Youbi, S. N. Baschel and A. Y. Obaid, Monatsh. Chem., 2007, 138, 853–857.

[29] M. Behpour, S. M. Ghoreishi, N. Mohammadi, N. Soltani and M. S. Niasari, Corros. Sci., 2010, 52, 4046–4057.

[30] I. B. Obot, E. E. Ebenso and M. M. Kabanda, J. Environ. Chem. Eng., 2013, 1, 431–439.

[31] S. E. Nataraja, T.V. Venkatesha and H.C. Tandon, Corros. Sci., 2012, 60, 214–223.

[32] E.E. Ebenso, Mater. Chem. Phys., 2003, 79, 58–70.

[33] N. A. Negm, Y. M. Elkholy, M. K. Zahran and S. M. Tawfik, Corros. Sci., 2010, 52, 3523–3536.

[34] G. Achary, H. P. Sachin, Y. A. Naik and T.V. Venkatesha, Mater. Chem. Phys., 2008, 107, 44–50.

[35] Y. Harinath, D. H. K. Reddy, B. N. Kumar, C. Apparao and K. Seshaiah, Spectrochim. Acta Part A, 2013, 101, 264–272.